Final Report • August 1993

SALI CHEMICAL ANALYSIS OF PROVIDED SAMPLES

Christopher H. Becker
Molecular Physics Laboratory

SRI Project 3557
Contract No. 1-1EH-46755
MP 93-164

Prepared for:

NASA
Marshall Space Flight Center
Huntsville, Al 35812

Attn.: Roger Linton
Mail Stop EH15

Final Report • August 1993

SALI CHEMICAL ANALYSIS OF PROVIDED SAMPLES

Christopher H. Becker

SRI Project 3557
Contract No. 1-1EH-46755
MP 93-164

Prepared for:

NASA
Marshall Space Flight Center
Huntsville, AL 35812

Attn.: Roger Linton
Mail Stop EH15

Approved:

Donald J. Eckstrom, Laboratory Director
Molecular Physics Laboratory

David M. Golden
Vice President
Physical Sciences Division

SRI International 333 Ravenswood Avenue • Menlo Park, CA 94025-3493 • (415) 326-6200 • FAX: (415) 326-5512 • Telex: 334486

SRI has completed the chemical analysis of all the samples supplied by NASA. The final batch of four samples consisted of

- Sample 1: 1-inch-diameter MgF_2 mirror, control 1200-ID-FL3
- Sample 2: 1-inch-diameter neat resin, PMR-15, AO171-IV-55, half exposed and half unexposed.
- Sample 3: 1-inch-diameter chromic acid anodized, EOIM-3 120-47 aluminum disc.
- Sample 4: AO-exposed and unexposed samples of fullerene extract material in powdered form. (These powders were pressed into In foil for analysis.)

Chemical analyses of the surfaces were performed by the surface analysis by laser ionization (SALI) method. The analyses emphasize surface contamination or general organic composition. SALI uses nonselective photoionization of sputtered or desorbed atoms and molecules above but close (~1 mm) to the surface, followed by time-of-flight (TOF) mass spectrometry. In these studies, we used laser-induced desorption by 5-ns pulse-width 355-nm light (10-100 mJ/cm^2) and single-photon ionization (SPI) by coherent 118-nm radiation (at $\sim 5 \times 10^5$ W/cm^2). SPI was chosen primarily for its ability to obtain molecular information, whereas multiphoton ionization (not used in the present studies) is intended primarily for elemental and small molecule information.

Although SPI by 118-nm (10.5-eV) light is considered a generally "soft" (nonfragmenting) form of radiation, stimulated desorption can cause fragmentation and can produce internally hot molecules that photofragment more easily than lower temperature sources of molecules. Typically, the low mass regions of the mass spectra contain some molecular fragment information.

Some other comments on the mass spectra are appropriate. The signals from the microchannel plate detector were recorded in analog fashion by a 100-MHz transient digitizer; thus the voltage signals are given as "relative intensity" and not as ion counts. For the two nonmetallic samples (samples 2 and 4), the surface was strongly absorbing; thus considerably less laser power was needed than for the two reflective metal samples (samples 1 and 3).

Some of the mass assignments have been marked on the figures, especially for the major peaks. Considerable effort could be devoted to mass interpretation. Some brief general interpretations follow.

For samples 1 and 3, a gas background (very low in intensity) has been subtracted in the plots; thus the baseline in these figures is at zero. The baseline in the sample 2 and 4 figures represents the dc offset value of the digitizer and is independent of the mass spectra.

Sample 1 shows a significant amount of organic contamination. The backside of the mirror gave only weak signals in comparison, although this assumes an equal temperature jump for the two different (though both largely nonabsorbent) surfaces. The fingerprint mass spectrum of Figure 1a can probably be used to identify the species present, although it is not obvious to the author what compound(s) is responsible. Some knowledge of the exposure chemical conditions and/or some literature examination for a variety of known materials is necessary.

For the unexposed neat resin (sample 2), direct ion signals (intense and broad mass peaks on a different mass scale--different time zero) are seen in Figure 2b and 2c in the low mass region; they are probably due to Na and K; their presence as direct ions is likely due to somewhat higher surface temperature being reached during the desorption laser pulse. Overall, there is marked enhancement in the amount of desorbing organic compounds in the exposed region. One possible explanation is that the polymers have been significantly fragmented by chemical cleavage. The 105 and 122 peaks are in common for both sides of the sample. The 149 m/z peak has many potential assignments but is often due to a phthalate ion. Peaks such as 149, 78, 91, and 105 are often associated with aromatic systems (see Figure 2a).

Sample 3 (Figures 3a and 3b) shows a reduction in hydrocarbon contamination after exposure (lower overall signal). There are some peaks in common for both sides of this sample. The unexposed side (Figure 3a) shows some aromaticity, such as phthalate ion at 149 (a common contaminant), 178 (often anthracene/phenanthrene), and 192 (=178 + methyl). Peaks such as 43, 57, 71, and 85 are alkane/alkene progressions, probably from side chains.

Sample 4 is based on a fullerene extract (not purified C_{60}). Only very modest oxidation is evident after oxygen exposure. The oxygen exposure has noticeably reduced the abundance of lower mass hydrocarbons (see Figures 4a-d).

In addition to these four samples, the Au mirror (EOIM-3 200-11, sample 4) was depth profiled again (see previous report). Argon ion sputtering was used together with photoionization with intense 355-nm radiation (35-ps pulsewidths). Figures 5a-d show depth profiles similar to those reported earlier, showing reproducibility. No chromium was found in the sample above noise level; its presence could at most be at the trace level. Somewhat more Ni appears to be present in the Au layer in the unexposed side, indicating thermal diffusion without chemical enhancement. The result of the presence of oxygen is apparently to tie-up/draw out the Ni as an oxide at the surface. The exposed region has a brownish tint appearance to the naked eye.

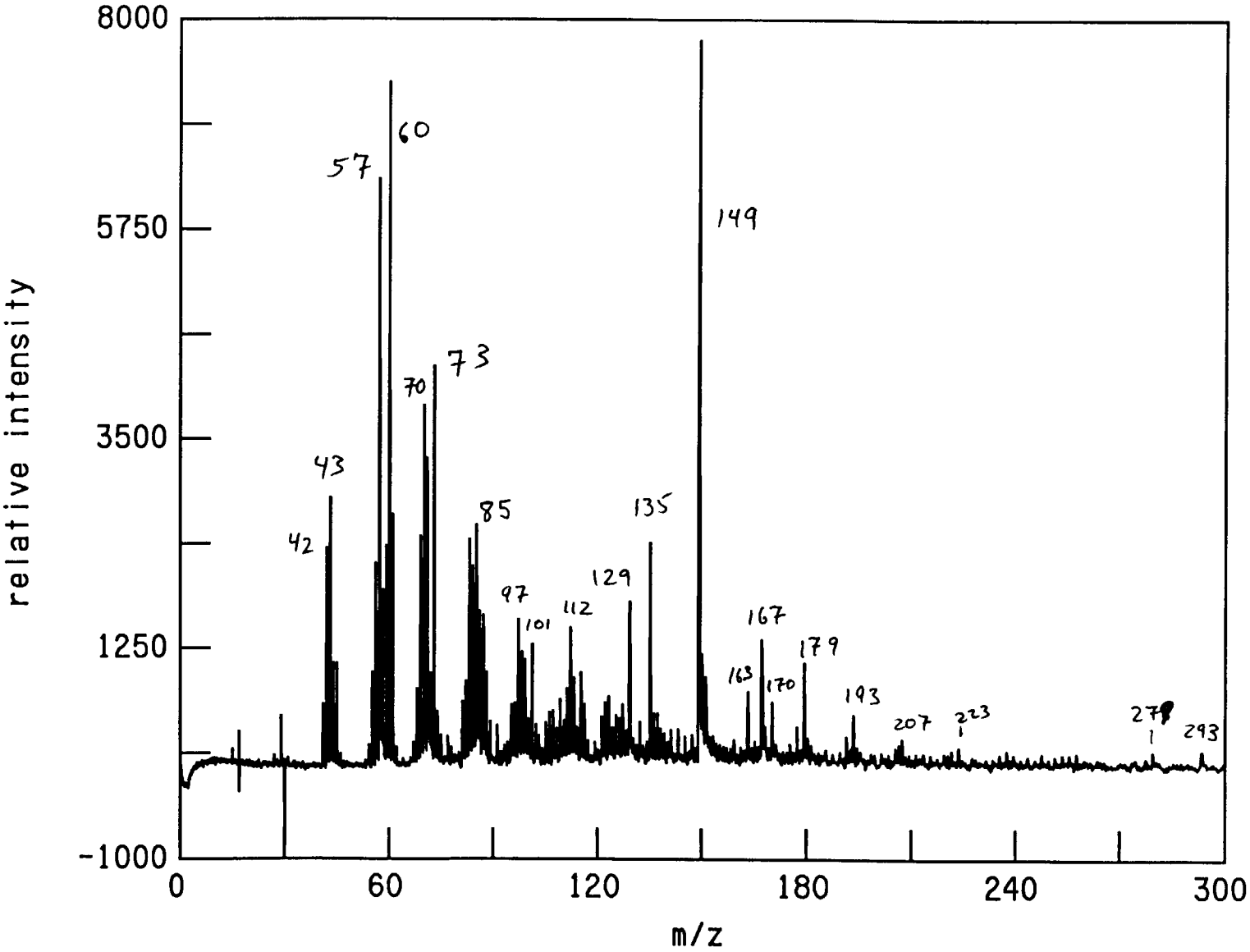

MgF2 mirror side up AU0307-AU0310, 118nm, 355nm desorption, 10db

Figure 1a

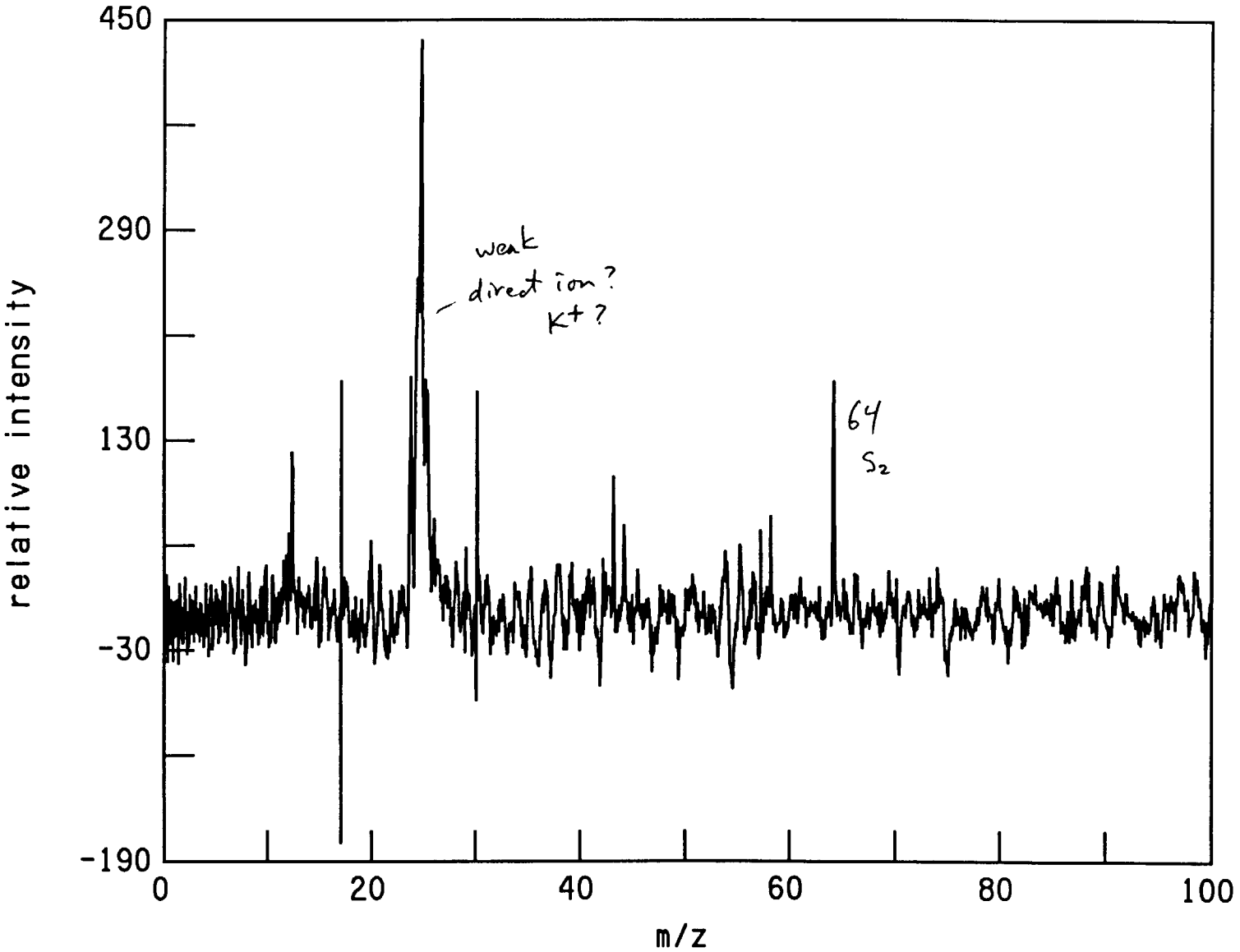

backside of MgF2 AU0309-AU0310, 118nm, 355nm desorption, 10db

Figure 1b

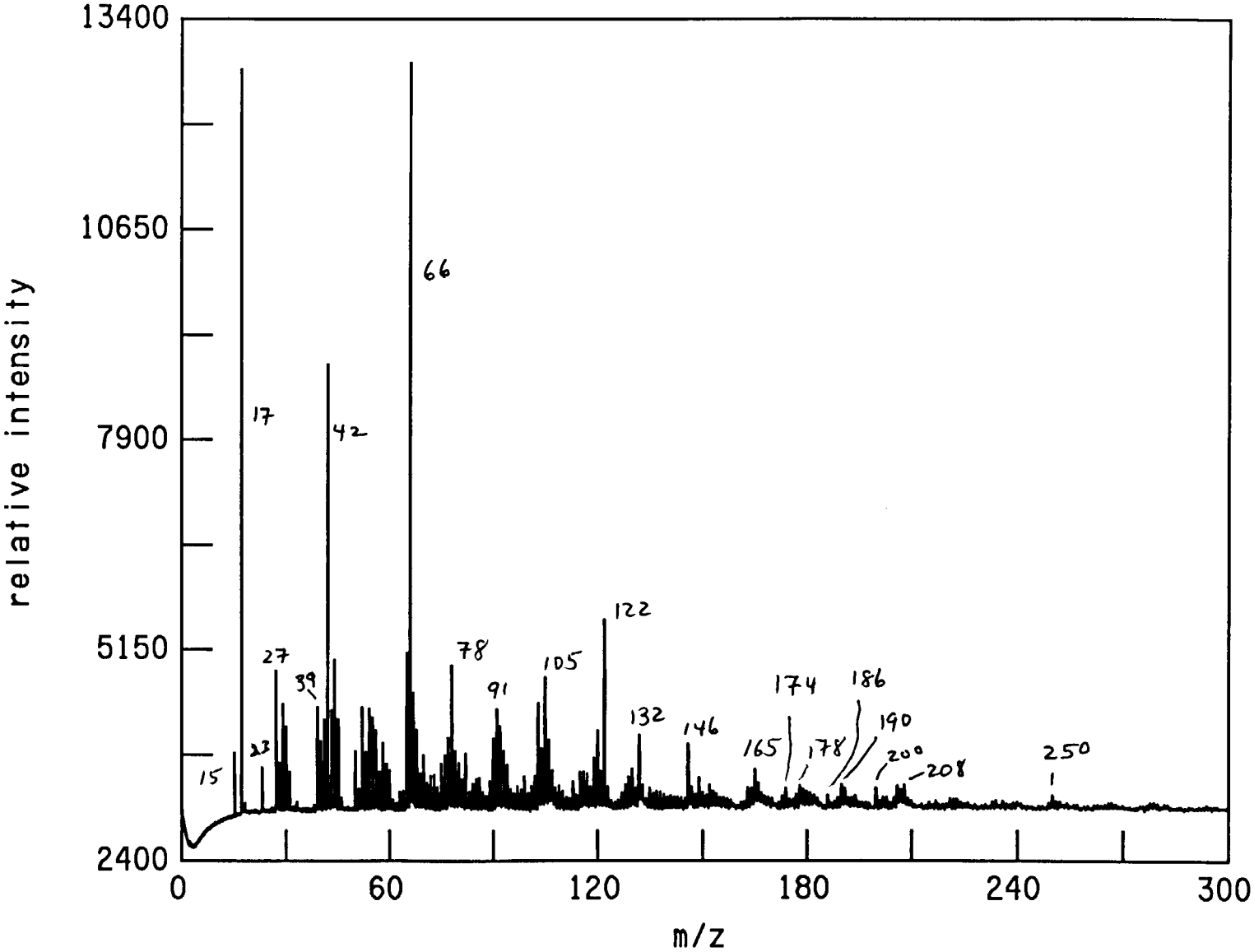

PMR-15 neat resin AU0403, 118nm, 355nm desorption, 20 db

exposed region

Figure 2a

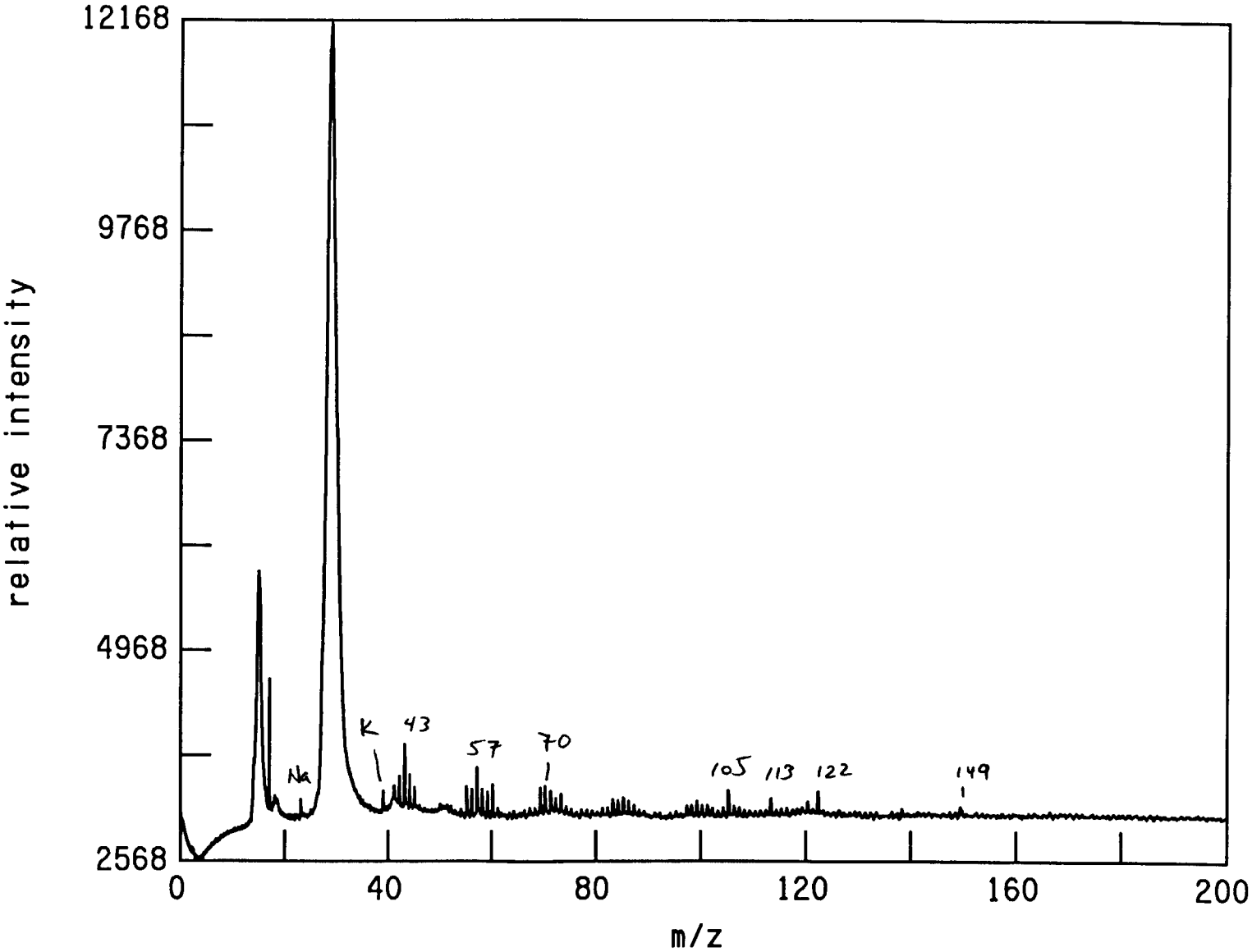

PMR-15 neat resin - unexposed AU0404, 118nm, 355nm desorption, 20db

Figure 2b

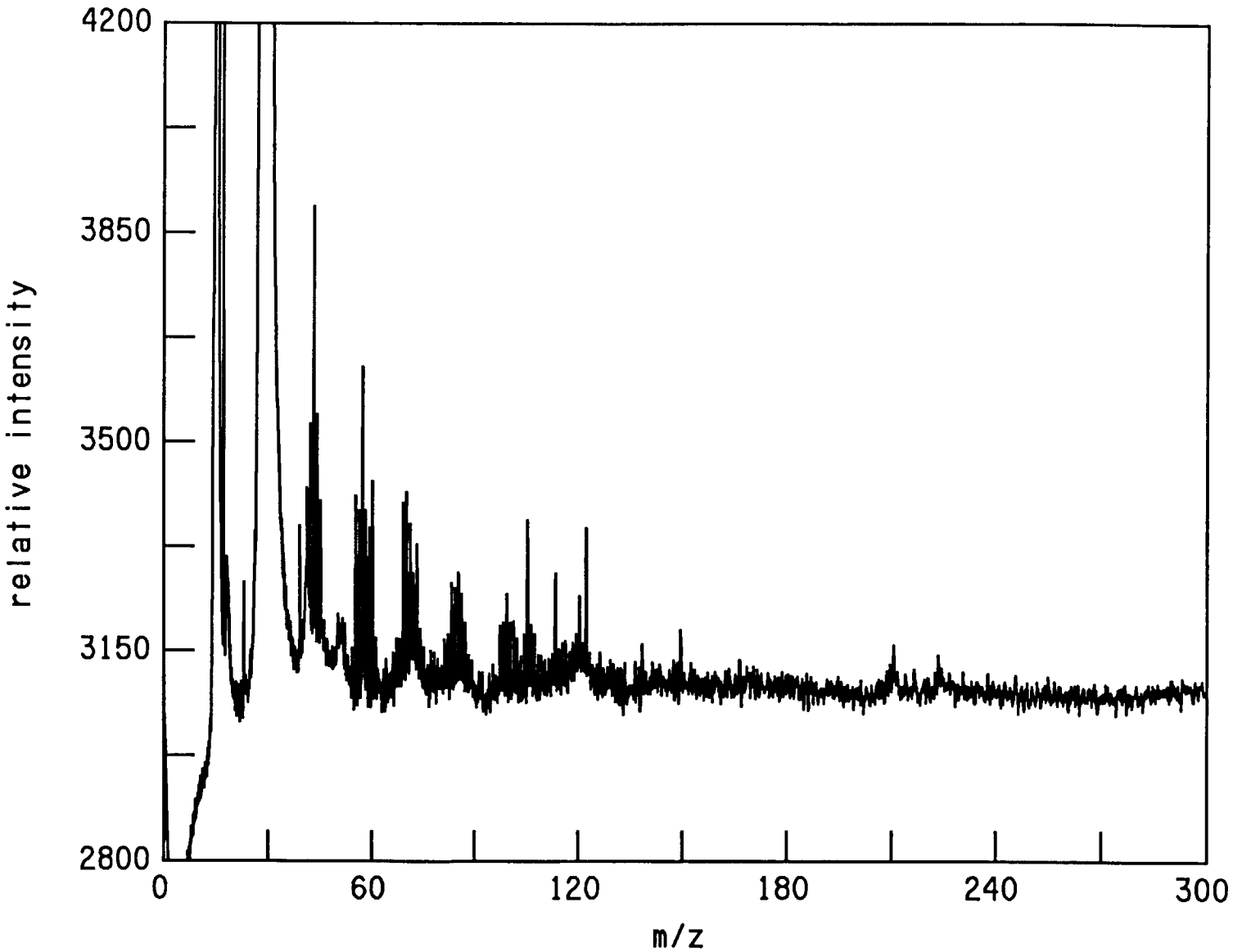

PMR-15 neat resin - unexposed AU0404, 118nm, 355nm desorption, 20db

(expanded vertical scale)
of Fig. 2b

Figure 2c

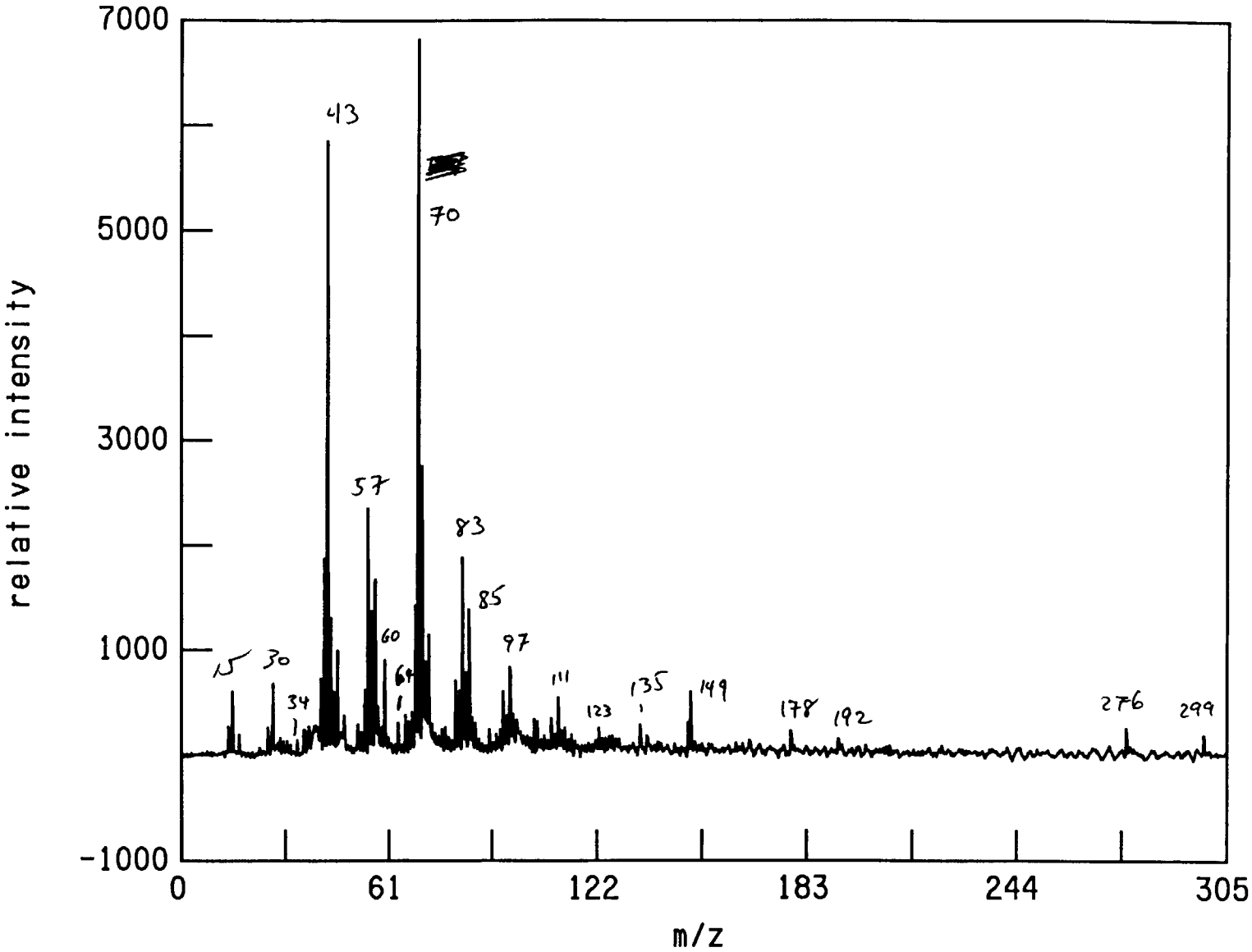

chromic acid anodized - unexposed AU0410-AU0411, 118nm, 355nm desorption, 10)t

Figure 3a

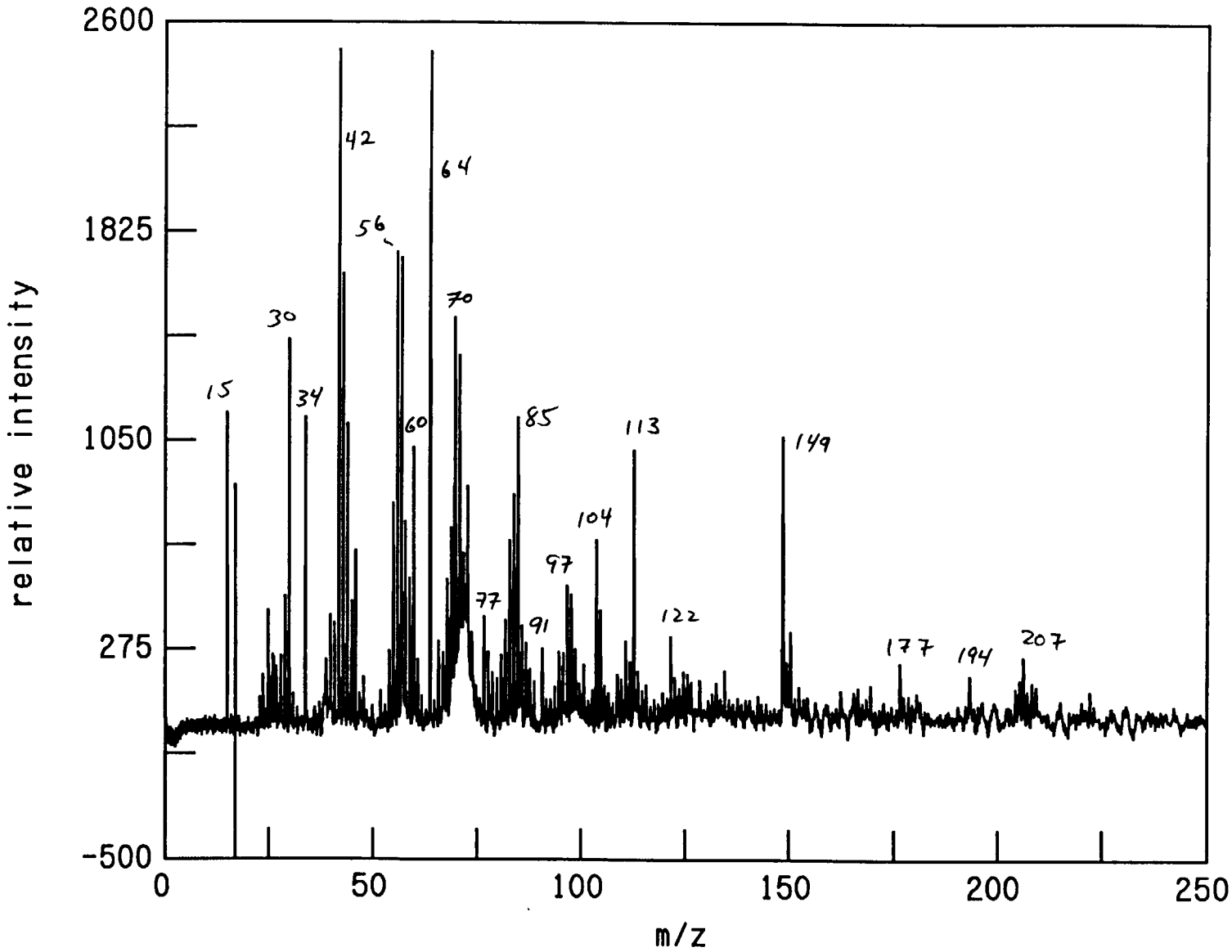

chromic acid anodized AU0408-AU0405, 118nm, 355 desorption, 10db exposed

Figure 3b

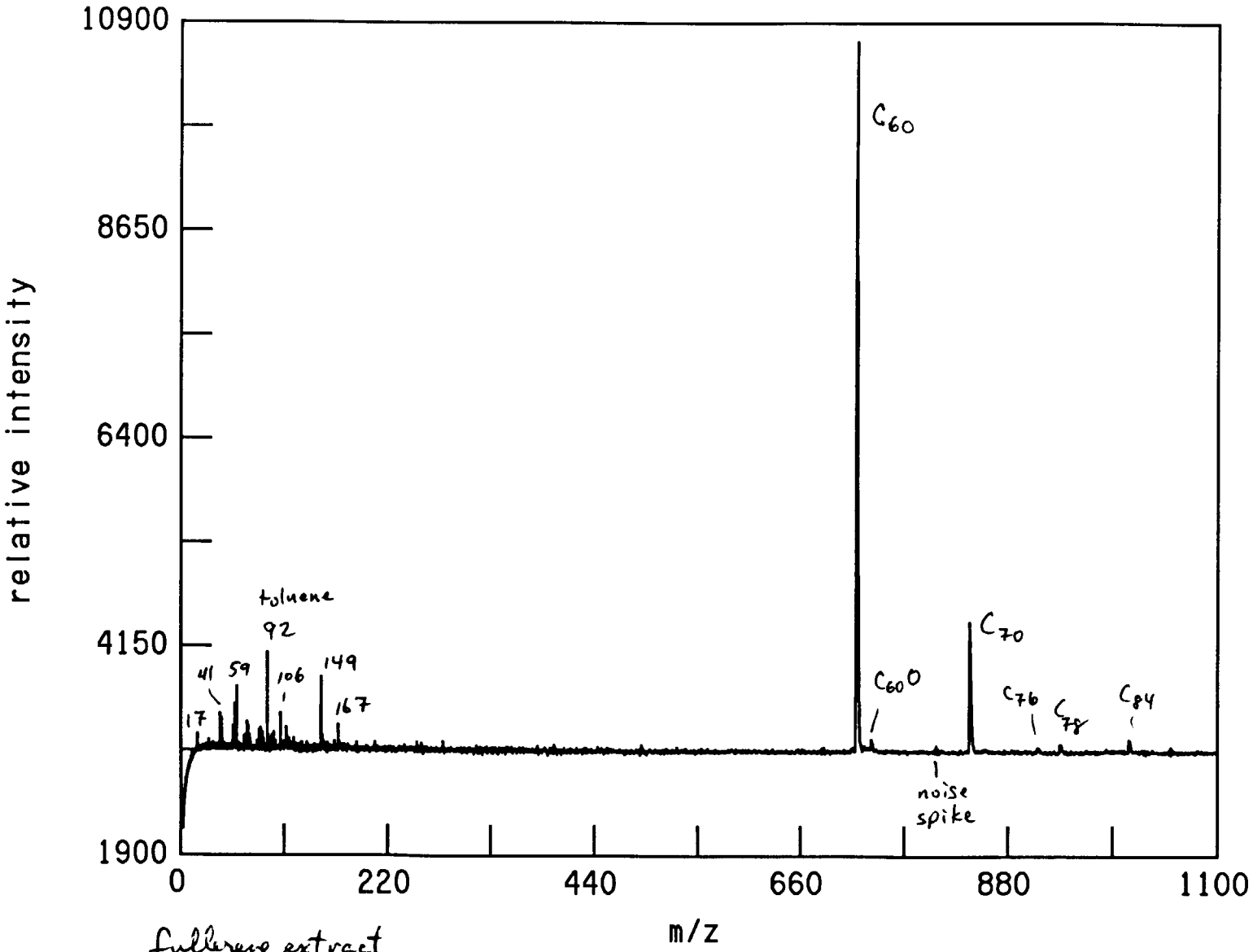

fullerene extract
exposed (C60) pressed into In AU0304, 118nm, 355nm desorption, 10db

Figure 4a

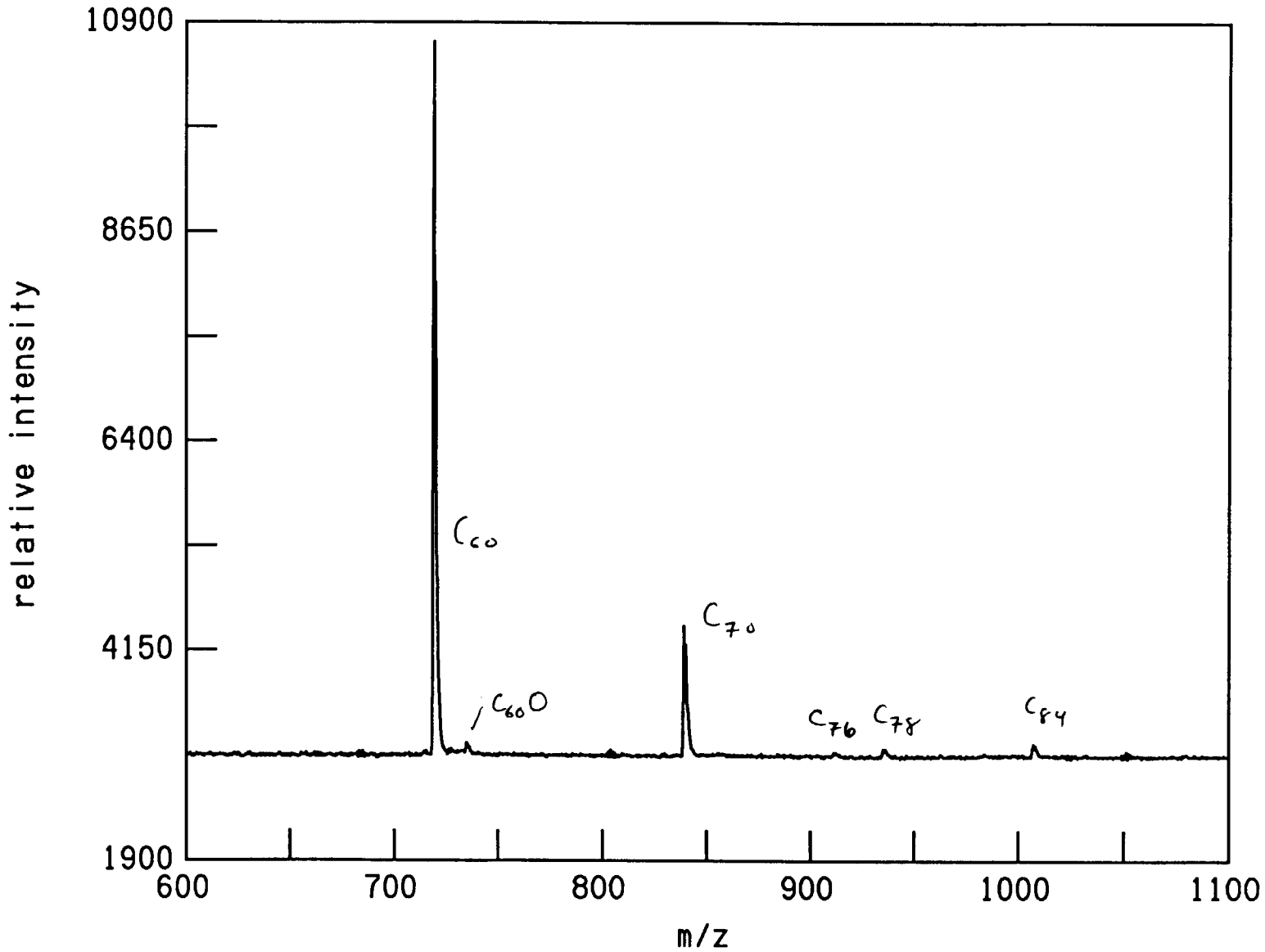

exposed C60 pressed into In AU0304, 118nm, 355nm desorption, 10db

Figure 4b

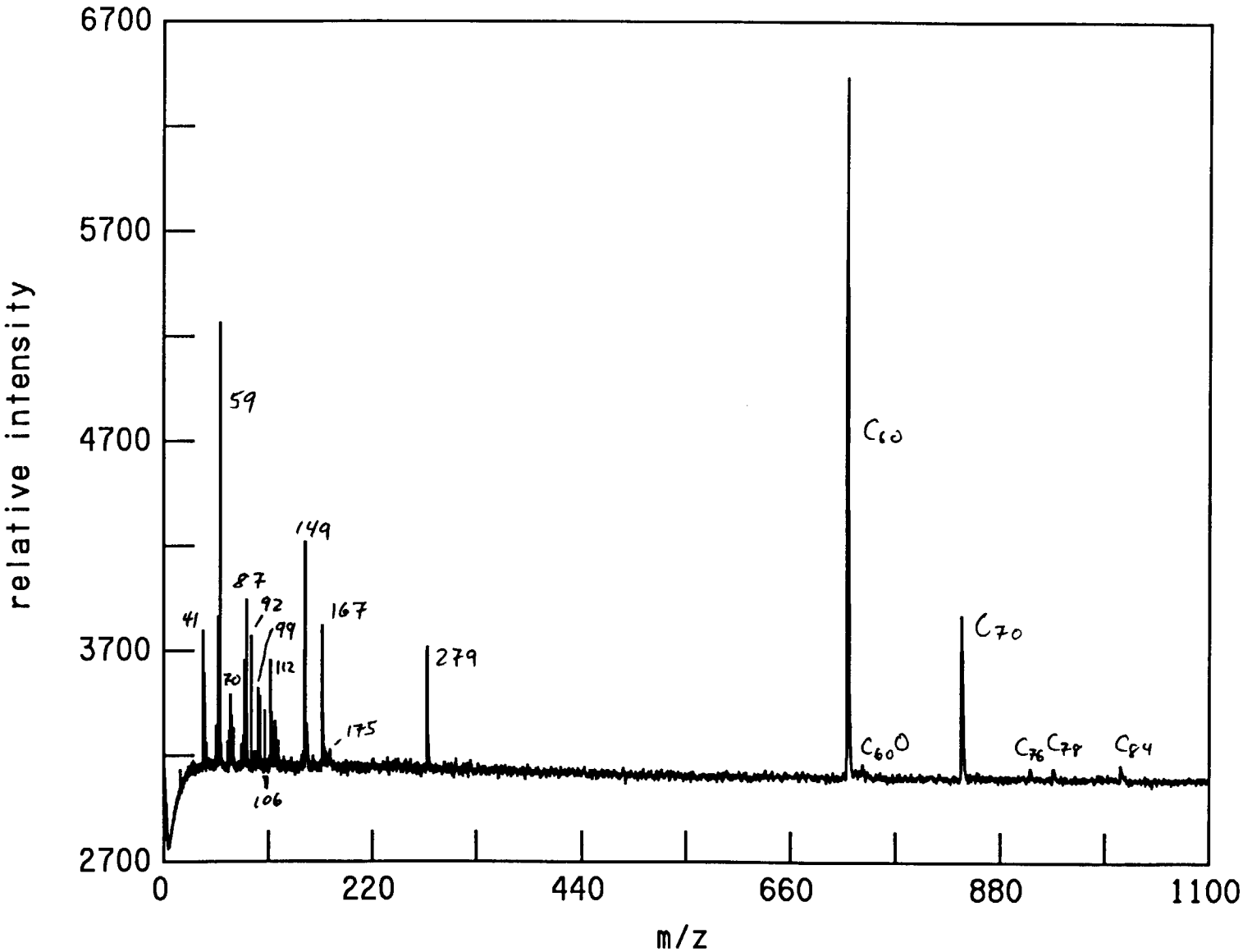

C60 pressed into In - control AU0306, 118nm, 355 desorption, 10db

Figure 4c

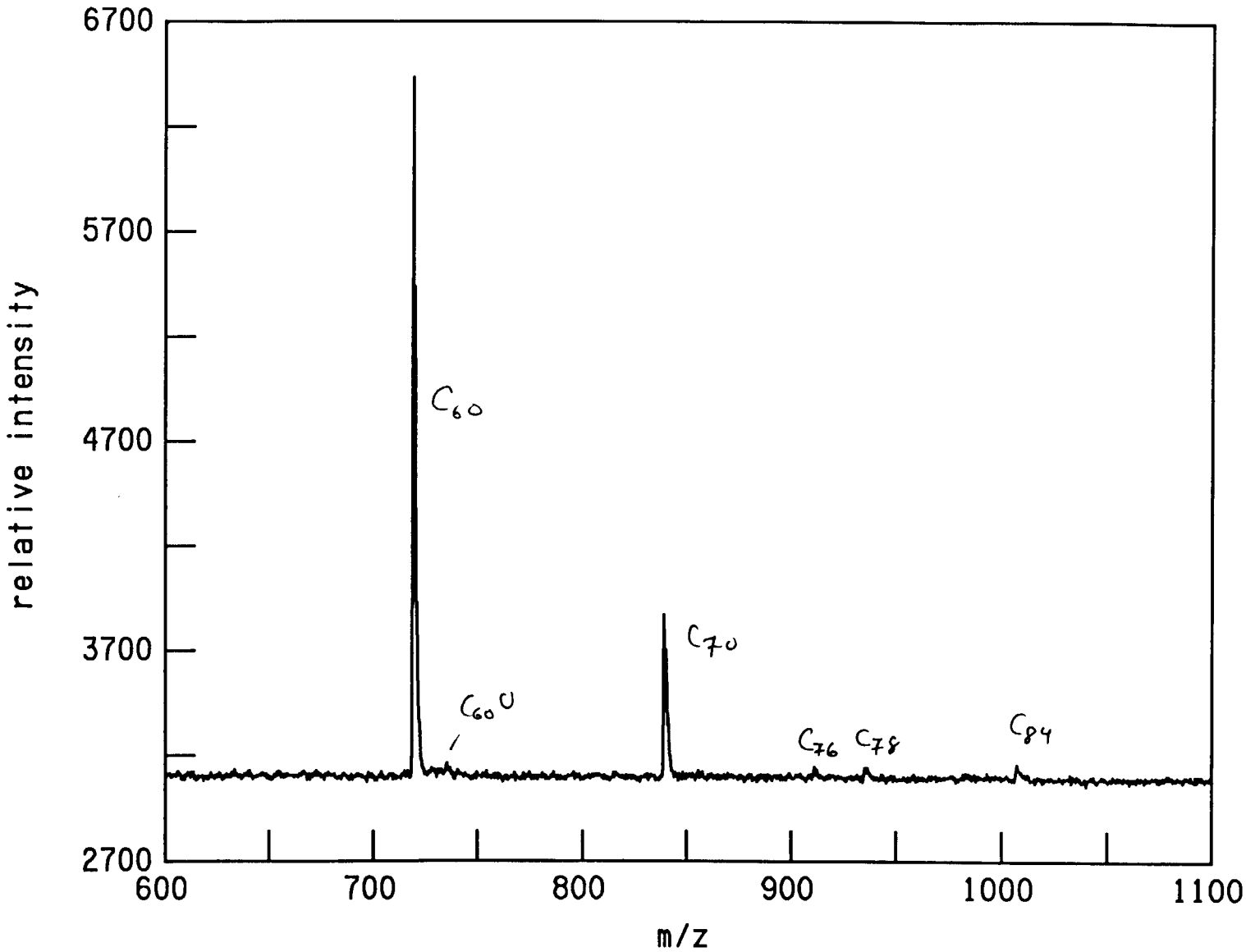

C60 pressed into In - control AU0306, 118nm, 355 desorption, 10db

Figure 4d

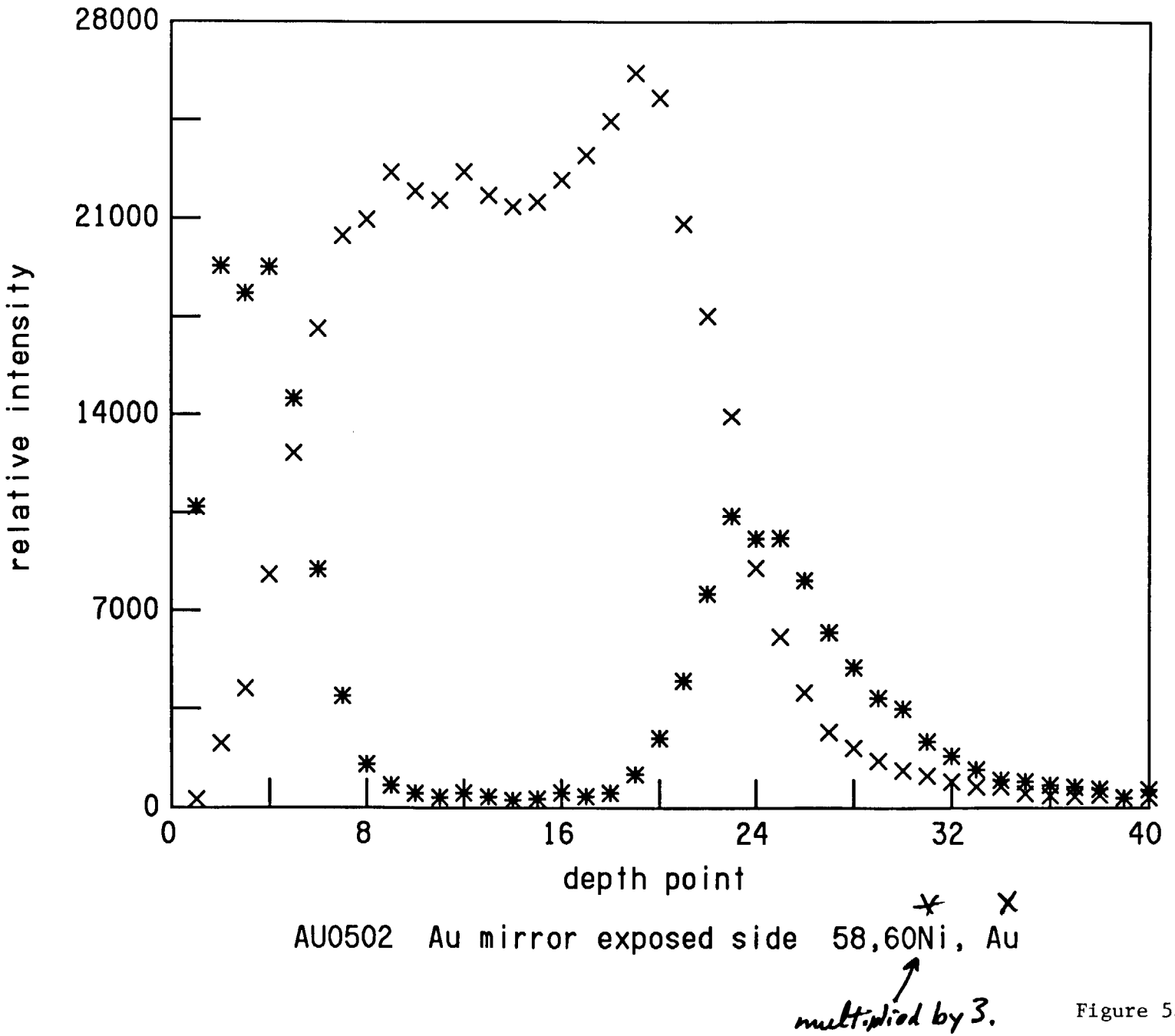

8/5/93

Figure 5a

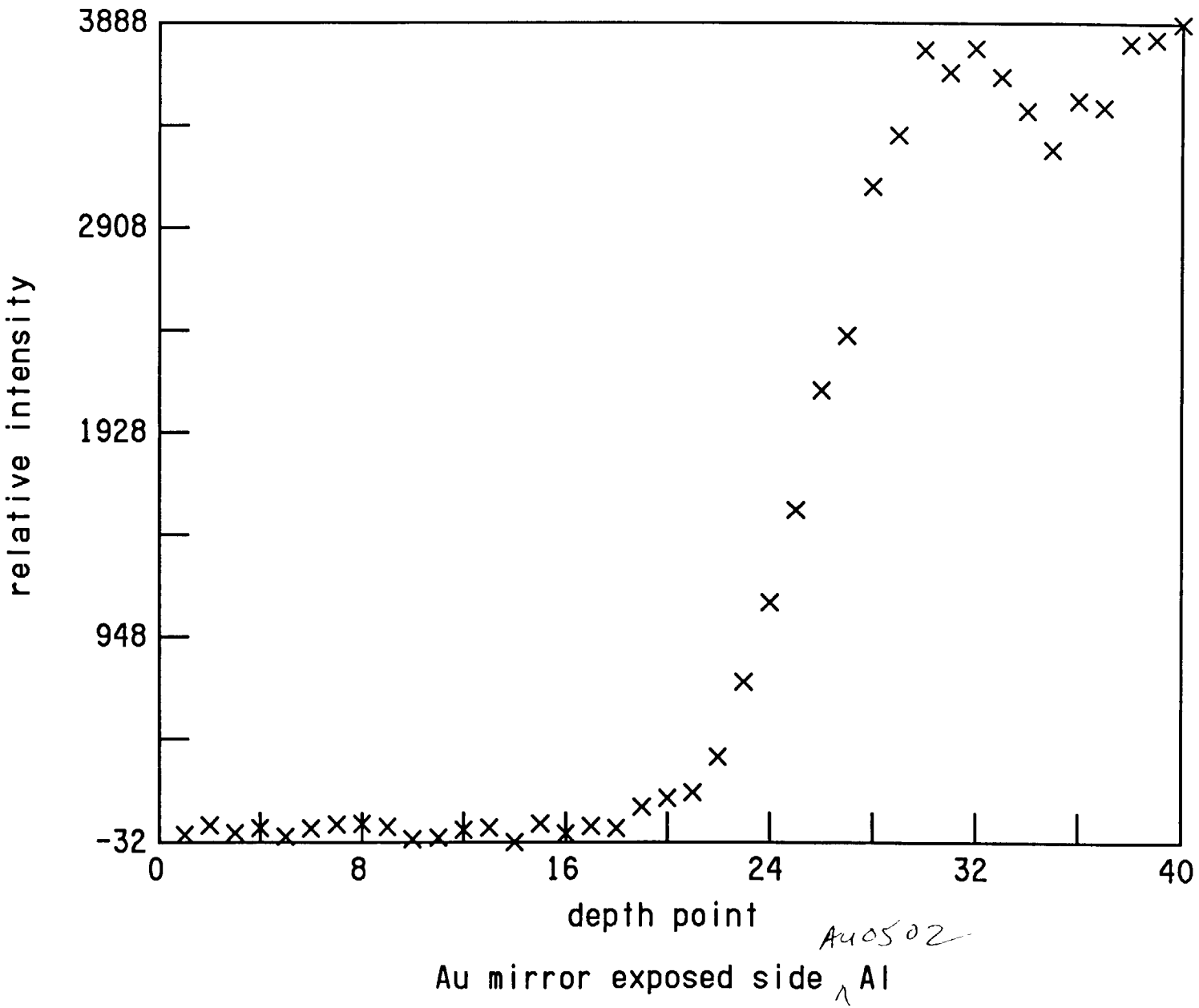

8/5/93

Figure 5b

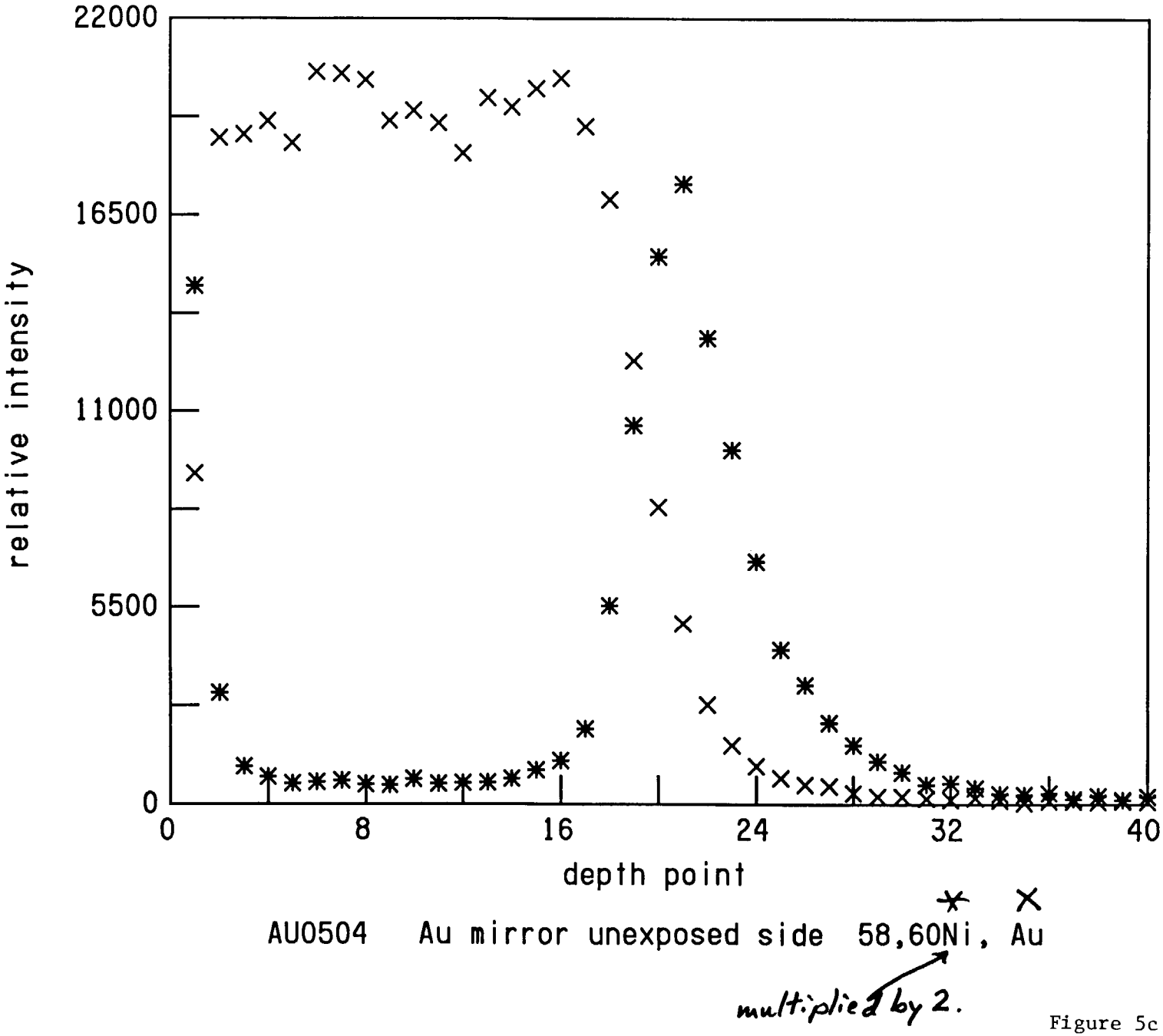

8/5/93

Figure 5c

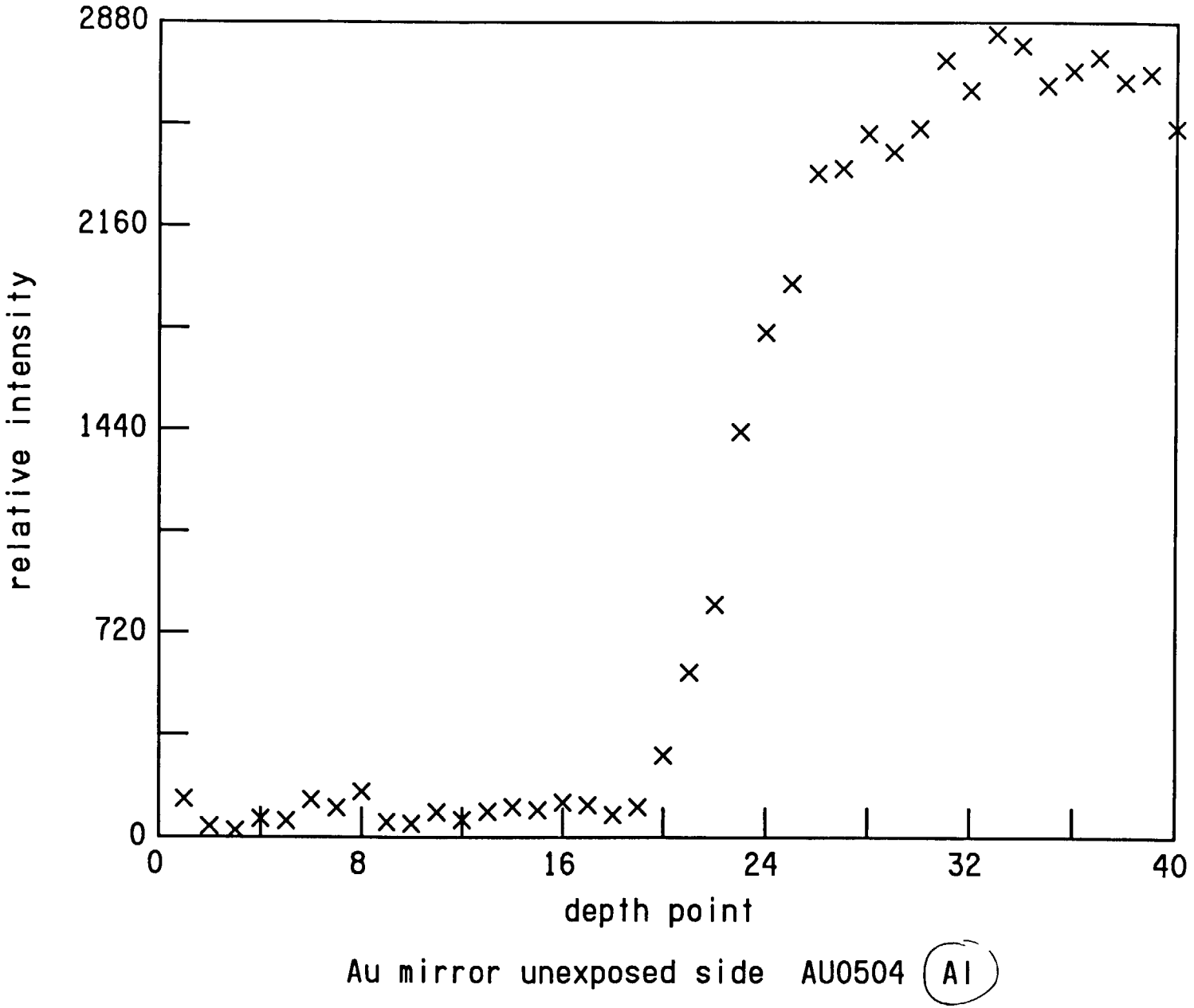

Figure 5d

8/5/93